Clim Dyn
DOI 10.1007/s00382-013-1986-3

Coupling of a regional atmospheric model (RegCM3) and a regional oceanic model (FVCOM) over the maritime continent

Jun Wei · Paola Malanotte-Rizzoli · Elfatih A. B. Eltahir · Pengfei Xue · Danya Xu

Received: 30 July 2013 / Accepted: 16 October 2013

Abstract Climatological high resolution coupled climate model simulations for the maritime continent have been carried out using the regional climate model (RegCM) version 3 and the finite volume coastal ocean model (FVCOM) specifically designed to resolve regions characterized by complex geometry and bathymetry. The RegCM3 boundary forcing is provided by the EMCWF-ERA40 re-analysis. FVCOM is embedded in the Global MITgcm which provides boundary forcing. The domain of the coupled regional model covers the entire South China Sea with its through-flow, the entire Indonesian archipelago with the Indonesian through-flow (ITF) and includes a large region in the western Pacific and eastern Indian oceans. The coupled model is able to provide stable and realistic climatological simulations for a specific decade of atmospheric–oceanic variables without flux correction. The major focus of this work is on oceanic properties. First, the coupled simulation is assessed against ocean-only simulations carried out under two different sets of air–sea heat fluxes. The first set, provided by the MITgcm, is proved to be grossly deficient as the heat fluxes are evaluated by a two-dimensional, zonally averaged atmosphere and the simulated SST have anomalous cold biases. Hence the MITgcm fluxes are discarded. The second set, the NCEP re-analysis heat fluxes, produces a climatological evolution of the SST with an average cold bias of ~ -0.8 °C. The coupling eliminates the cold bias and the coupled SST evolution is in excellent agreement with the analogous evolution in the SODA re-analysis data. The detailed comparison of oceanic circulation properties with the International Nusantara Stratification and Transport observations shows that the coupled simulation produces the best estimate of the total ITF transport through the Makassar strait while the transports of three ocean-only simulations are all underestimated. The annual cycle of the transport is also very well reproduced. The coupling also considerably improves the vertical thermal structure of the Makassar cross section in the upper layer affected by the heat fluxes. On the other hand, the coupling is relatively ineffective in improving the precipitation fields even though the coupled simulation captures reasonably well the precipitation annual cycle at three land stations in different latitudes.

Keywords Regional atmosphere–ocean coupled model · Air–sea interactions · Climate variability · Southeast Asian maritime continent

J. Wei (✉)
Peking University, Beijing, China
e-mail: junwei@pku.edu.cn

J. Wei · P. Malanotte-Rizzoli · E. A. B. Eltahir · P. Xue · D. Xu
Singapore-MIT Alliance for Research and Technology, Singapore, Singapore

P. Malanotte-Rizzoli · E. A. B. Eltahir · P. Xue
Massachusetts Institute of Technology, Cambridge, MA, USA

1 Introduction

The Maritime Continent is a highly complex region with relatively large ocean coverage and chains of islands of different sizes separated by straits interconnecting different sub-basins and local seas. The domain of the Maritime Continent and surrounding regions is shown in Fig. 1. One significant challenge in simulating atmospheric variables

Published online: 21 November 2013

such as rainfall over the region is how to represent accurately the ocean–atmosphere–land interactions for a range of spatial and temporal scales. Due to the large ocean areas, two-way air–sea feedbacks processes will be important in modeling the climate of the Maritime Continent, since the local sea surface temperature (SST) is a major variable determined by surface heat fluxes and rainfall variability, which are in turn shaped by SST. Uncoupled atmospheric models prescribe spatially and temporally interpolated SST fields as lower boundary conditions, while uncoupled ocean models prescribe surface wind stress and heat and moisture fluxes interpolated to the ocean grid. The latter ones are calculated either using bulk formulae or, more recently, taken from community atmospheric datasets such as the NCEP reanalysis (Kalnay et al. 1996). However, atmosphere-only or ocean-only configurations ignore the two-way dynamical interactions that occur at the ocean–atmosphere interface. A coupled ocean–atmosphere model should be capable of simulating more realistic dynamics close to the ocean surface, where the ocean–atmosphere exchanges take place. In particular, for the Maritime Continent the coupled domain should cover the entire South China Sea (SCS) with its through-flow (SCSTF) and the Indonesian Through-flow (ITF) through which the transfer of tropical/subtropical water occurs from the western Pacific to the Indian ocean as this transfer is closely linked by air–sea fluxes to coupled climate modes of interannual/decadal variability such as El Nino-Southern Oscillation (ENSO).

During the last two decades several research groups were successful in coupling regional models of the atmosphere and ocean, many of them in Europe (for a recent review of regional climate change projections in the Mediterranean region see Gualdi et al. 2012). Fewer coupled regional ocean–atmosphere models have been developed for Asian domains. Here we focus on the latter studies and specifically on those most relevant to our work summarizing their results.

Ren and Qian (2005) developed a coupled regional air–sea model to simulate the East Asian Summer monsoon in 1998. The model domain differs from that shown in Fig. 1 as it excludes almost completely the Indonesian archipelago with the southern boundary at 5°S. The atmospheric component is the regional climate model named (P-σRCM) and the oceanic component is based on the Princeton Ocean Model (POM). The authors also carried out ocean-only simulations with the uncoupled POM. The major difference between the uncoupled and coupled results (and observations) is a cold tendency of the simulated sea surface temperatures (SST) in the coupled model system, which does not reach a stable climate but exhibits instead a cold drift away from the observed climatology.

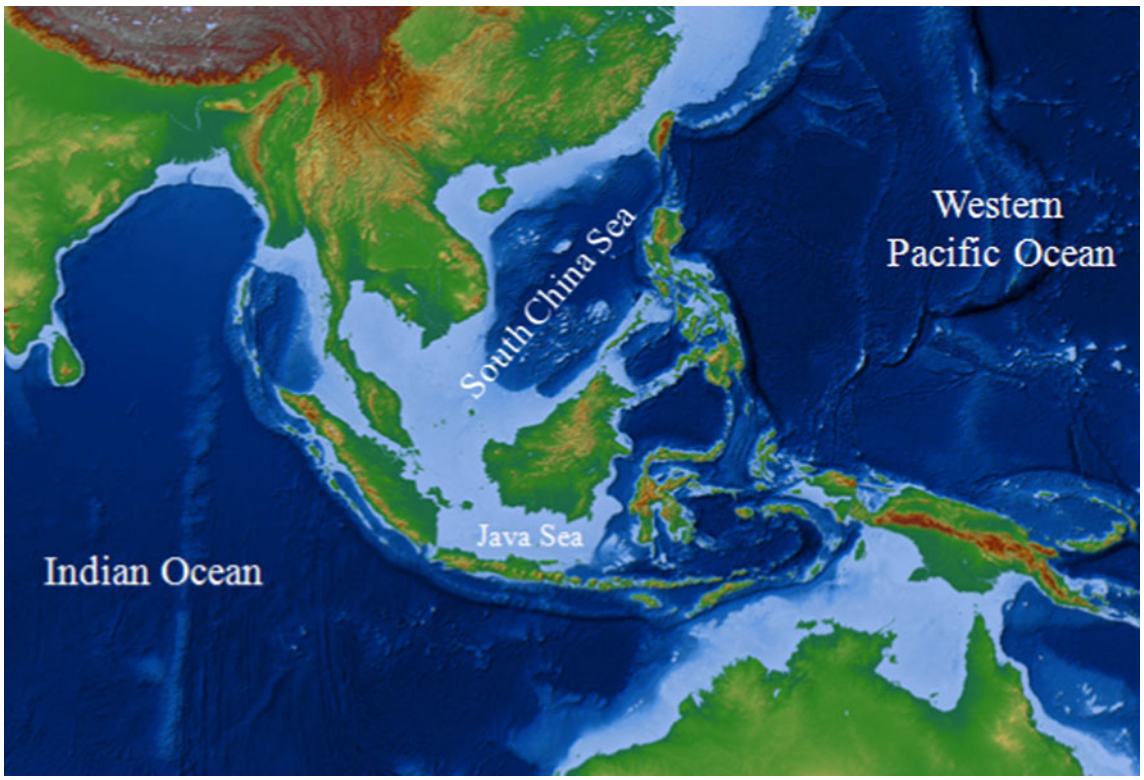

Fig. 1 The Maritime Continent

This cold drift is attributed to the disagreement of the surface heat fluxes produced by the atmospheric model with those required by POM. A similar result was found by Fang et al. (2009b) who developed a regional air-sea coupled model to simulate the summer climate over East Asia in 2000. Their domain also excludes the Indonesian archipelago but includes a large area in the western Pacific ocean, with the southern boundary located at the equator. In this study the atmospheric component is the Regional Integrated Environment Model System (RIEMS) and the ocean one is again POM. The coupled simulations produced a climate drift especially for SST biases, and sensitivity experiments show that the SST biases are again due to the mismatch of the surface heat fluxes produced by RIEMS with those required by POM. Li and Zhou (2010) developed a regional air–sea model over East Asia. Their model domain is very similar to that of the previous study, but the southern boundary is at 10°N. The atmospheric component is RegCM3 (Pal et al. 2007) and the oceanic component the Hybrid Coordinate Ocean Model (HYCOM). A 20-year coupled integration was carried out to reproduce the present climate of the region. Again the coupled simulation produced a cold bias of $\sim$2 °C in the SST. This cold bias was removed through a heat flux adjustment for the solar short-wave radiation to keep the SST close to the observations. Zou and Zhou (2011) coupled RegCM3 with POM over the western North Pacific. Their domain is rather different from those of the previous works as well as from ours. The atmospheric component is RegCM3 and the oceanic one POM, and this regional coupled model is named ROAM. Its performance was assessed by simulating the 1998 Summer monsoon. Again a cold bias is evident in the SST, and this is a common feature of previous ROAM simulations over the Asian Australian Summer monsoon region, as discussed by the authors. Zou and Zhou (2011) attribute the SST cold biases to the overestimation of convection frequency by the atmospheric model, at least partially.

The most important previous work on the Indonesian Maritime continent is the coupled regional model developed by Aldrian et al. (2005) which used the Max Planck Institute Regional Coupled Model (RCM, Aldrian et al. 2004) and the Max Planck Institute Ocean Model (MPI-OM). More specifically, the atmospheric component is the Regional atmosphere Model (REMO); the ocean component is the global ocean MPI-OM; the coupling between the two is accomplished by the OASIS coupler (Terray et al. 1999, version 2.3; Valcke et al. 2000, version 2.4). Differently from the previously quoted studies, in which the coupled models exhibit a cold drift/bias from the observed climatology and often correct for it through a flux correction, in the work by Aldrian et al. (2005) the coupled model is able to simulate stable and realistic rainfall variabilities without flux correction. Their results show improved performance after coupling, i.e. a remarkable reduction of overestimated rainfall over the sea for the atmospheric component and of warm SST biases for the ocean component. Even though the work by Aldrian et al. (2005) contains a significant section for the ocean, the major emphasis of the paper is on rainfall as explicitly stated in the title.

Some important differences exist between our work and that by Aldrian et al. (2005) which we now summarize. First, the atmospheric and oceanic models. We use the Regional Atmospheric Model RegCM3 adapted to the domain of the Maritime Continent shown in Fig. 2a (Gianotti et al. 2012). The ocean model is the finite volume coastal ocean model (FVCOM, Chen et al. 2003, 2006a, b) which is embedded in the Global MIT general circulation model (MITgcm). Second, MPI-OM in the high-resolution model used in Aldrian et al. (2005) has a maximum resolution of $\sim$15 km near the poles located inside the China and Australia interiors, much coarser elsewhere especially in the ITF straits. FVCOM resolution is $\sim$7 km. on the shelves, continental slopes and in all the local seas and straits of the ITF. Third, the coupled domain is very different. In Aldrian et al. (2005) REMO divides the MPI-OM into two sub-domains, coupled and uncoupled. The coupled domain is the REMO domain, 19°S–8°N; 91°E–141°E (Fig. 2, lower panel, Aldrian et al. (2005)). Our ocean-only and coupled domains, shown in Fig. 2b, are the same and cover 20°S–30°N; 85°–140°E. Our domain includes a large region of the western tropical-subtropical Pacific from which coupled modes of ocean–atmosphere interannual and decadal variability are transmitted from the Pacific to the Indian ocean through the Indonesian Through Flow (ITF) and South China Sea Through Flow (SCSTF, Gordon 2005; Gordon et al. 2012). Finally, the simulation periods of the two works are very different. In Aldrian et al. (2005), the coupled model simulation is analyzed for the period 1979–1993. In our work we focus on simulating the climatological atmospheric/oceanic patterns. From the global MITgcm, in which the ocean model is embedded, we have available 4 decades of weekly averages of atmospheric/oceanic variables, 1960–2000. The two decades of 1960–69 and 1990–99 have been investigated in ocean-only simulations by Xu and Malanotte-Rizzoli (2013) using the same domain/grid of Fig. 2b. Here we extend the investigation to the decade 1970–1979 with both the coupled and ocean-only models.

The first two goals of this work are obviously similar to those of Aldrian et al. (2005): to analyze the performance of our very-high resolution coupled climate model; to compare the results of the coupled simulations with those of the uncoupled individual components, the atmosphere-only and ocean-only simulations as well as with

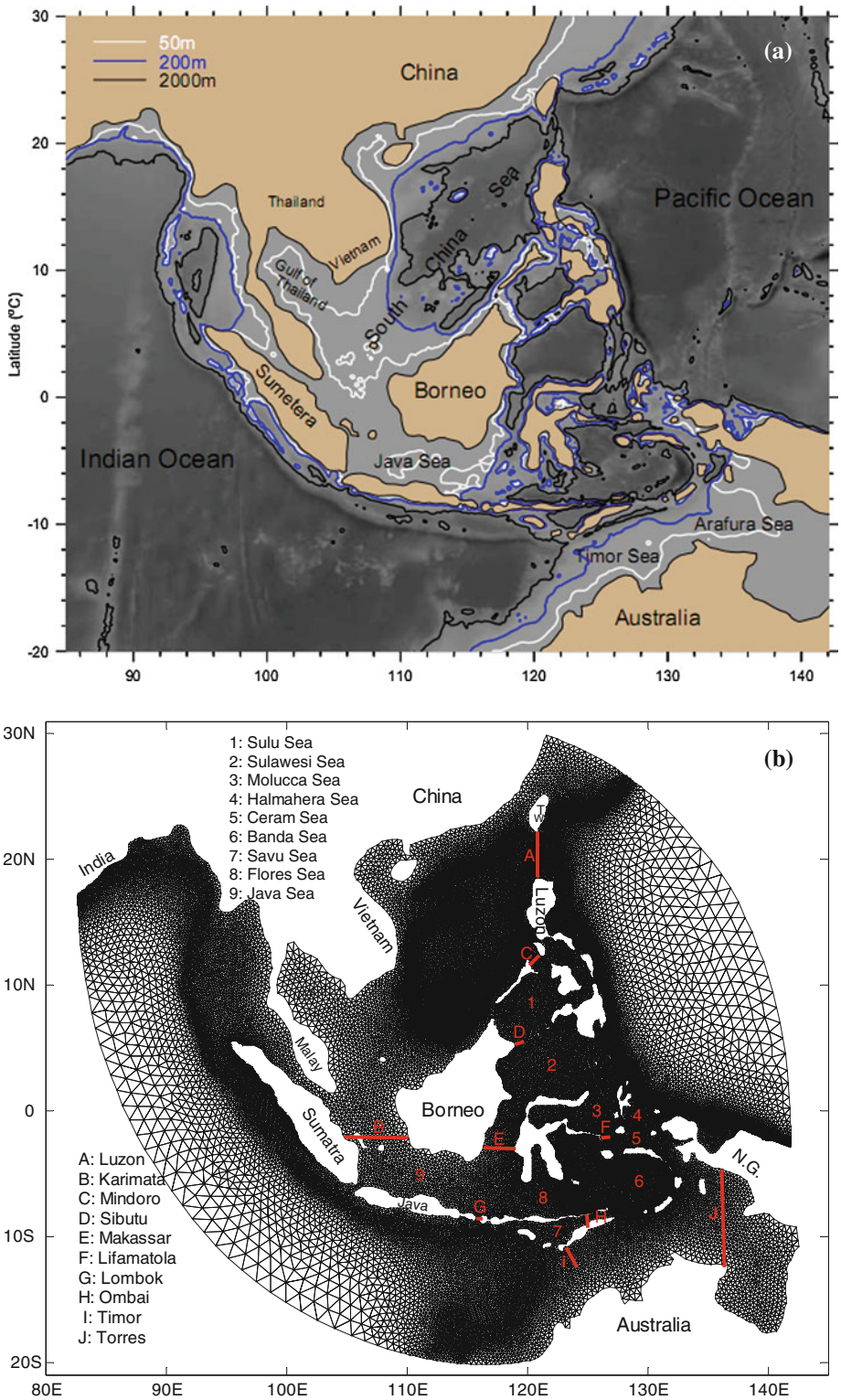

Fig. 2 Model domain: **a** RegCM3 domain with the 50, 200 and 1,000 m isobaths and **b** FVCOM domain with the unstructured grid, adapted from Xu and Malanotte-Rizzoli (2013). The various straits connecting the different seas of the Indonesian archipelago are marked by letters and the seas by numbers, with the names in the inset

climatological observations. However, as our major focus is on oceanic variables, our most important goal is to compare oceanic circulation properties from the ocean-only simulations for the three decades of the 60s, 70s, 90s with the coupled simulation of the 70s and the observations provided by recent experiments covering the ITF.

The paper is organized as follows. Section 2 describes the data used, the models and their set-up. Section 3 presents the results of the coupled simulation, their comparison with the atmosphere-only, ocean-only simulations and observations. Section 4 provides first a short discussion of the oceanographic properties of the SCS/ITF system and of

their importance for the Indonesian climate; and then a comparison of the coupled and ocean-only simulations with the available observations. Finally Sect. 5 gives concluding remarks and highlights the major findings.

2 Data and model set-up

2.1 Data

A number of different datasets are used in this study. For the atmospheric regional model RegCM3 the forcing from the 40-year European Centre for Medium Range Weather Forecasts (ECMWF) re-analysis (ERA-40, Uppala et al. 2005) at 6 h frequency is used to drive RegCM3 at the lateral open boundaries. The forcing includes the surface pressure and wind components, air temperature, vertical velocity, relative humidity, geopotential at all vertical sigma levels. In the atmosphere-only simulations the surface SSTs are provided by the Global Sea-Ice and Sea Surface Temperature (GISST) analysis which gives global SST monthly averages on a $1^\circ \times 1^\circ$ grid from 1971 to 2003. The GISST SST are produced from in situ measurements from ships and buoys infilled using Empirical Orthogonal Function (EOF) interpolation (Rayner et al. 1996). They are interpolated to the RegCM3 horizontal grid. The GISST SST are not used in the coupled and ocean-only simulations for reasons discussed in the following. For the comparison between the coupled and atmosphere-only simulations we use the Tropical Rainfall Measuring Mission (TRMM) dataset (Huffman et al. 2007) for precipitation and the NCEP re-analysis for winds and heat fluxes. The NCEP dataset (Kalnay et al. 1996) has the coarse resolution of $2.5^\circ \times 2.5^\circ$ in longitude and latitude for the period 1948–2008 and is interpolated to the RegC3 and FVCOM grids.

For the comparison of the SSTs from the coupled and ocean-only simulations we use instead the SODA re-analysis (Carton et al. 2000a, b) as the reference dataset. In the atmosphere-only simulation the SSTs are just the lower boundary condition for RegCM3, and not a dynamically active field. A simple interpolation of surface data suffices. In the coupled and ocean-only simulations on the other hand the SSTs are a dynamically active field as ocean temperature is a prognostic variable of the ocean model. The SSTs are therefore determined not only by air–sea fluxes but, equally importantly, by ocean circulation processes, i.e. vertical/horizontal advection and diffusion. The SODA re-analysis is a data assimilation product, combining all the worldwide available observations at all ocean depths with the GFDL POP (Parallel Ocean Program) global ocean circulation model for the period 1871–2008, hence taking into account ocean dynamical processes.

2.2 The regional atmospheric model RegCM3

The regional climate model (RegCM) was originally developed at the National Center for Atmospheric Research (NCAR) and is now maintained by the International Center for Theoretical Physics (ICTP). It is a three-dimensional, hydrostatic, compressible, primitive equation, σ-coordinate regional climate model, with a constant resolution of 60 km. The dynamical core of RegCM Version 3 (RegCM3) is based on the hydrostatic version of the Pennsylvania State University/NCAR Mesoscale Model Version 5 (MM5; Grell et al. 1994) and employs NCAR's Community Climate Model Version 3 (CCM3) atmospheric radiative transfer scheme (described in Kiehl et al. 1996). Planetary boundary layer dynamics follow the non-local formulation of Holtslag et al. (1990; described in Giorgi et al. 1993). Ocean surface fluxes are handled by Zeng's bulk aerodynamic ocean flux parameterization scheme (Zeng et al. 1998) and are computed from prescribed SSTs. RegCM3 has been adapted to the domain of the Maritime Continent shown in Fig. 2a for the study of convective cloud and rainfall processes (Gianotti et al. 2012) to whom the reader is referred for details. The model horizontal resolution is set to 60 km. with 18 uniform vertical sigma layers, from the ground surface to the 50-mb level.

2.3 The regional ocean model FVCOM (finite volume coastal ocean model)

FVCOM is a three dimensional, free surface, primitive equation, finite volume coastal ocean model, originally developed by Chen et al. (2003). The model adopts a non-overlapping unstructured (triangular) grid and finite volume method. The unstructured grid combines the advantages of finite-element methods for geometric flexibility and finite-difference methods for computational efficiency. FVCOM solves the momentum and thermodynamic equations using a second order finite-volume flux scheme that ensures mass conservation on the individual control volumes and the entire computational domain (Chen et al. 2006a, b). The Mellor and Yamada level 2.5 turbulent closure scheme is used for vertical eddy viscosity and diffusivity (Mellor and Yamada 1982) and the Smagorinsky turbulence closure for horizontal diffusivity (Smagorinsky 1963). For details of FVCOM see http://fvcom.smast.umassd.edu/FVCOM/index.html.

The flexible unstructured grid is capable of designing a model domain with varied resolutions to fully resolve its complex geometry and bathymetry, presented in Fig. 2a. Figure 2b shows the unstructured grid with 67,716 non-overlapping triangular cells and 34,985 nodes. The domain covers the entire SCS and Indonesian archipelago, including large sections in the western Pacific and eastern

Indian oceans. The open eastern and western boundaries have purposely been chosen to be in the two ocean interiors to prevent boundary effects, such as spurious wave reflection, from affecting the interior circulation. The sigma coordinate is used in the vertical and is configured with 31 layers (finer at surface and coarser at depth), which provides a vertical resolution of <1 m near surface on the shelf, and ~10 m in the open ocean. The water depth at each grid point is interpolated from ETOPO5 (Fig. 2a). The horizontal resolution varies from ~7 km on the shelves, continental slopes and in the straits, to ~10 km along the coastlines, to ~50 km in the deep SCS and ~200 km along the open boundaries.

2.4 The global MIT general circulation model MITgcm

FVCOM is embedded in the global ocean MITgcm (Hill and Marshall 1995; Marshall et al. 1997) which is a component of the MIT Integrated Earth System Model. The latter one comprises the ocean GCM, a primitive equation, three-dimensional model with the resolution of 2.5° × 2° in longitude and latitude respectively and 22 vertical z-levels (layer thickness ranging from 10 to 765 m). It includes a prognostic carbon model. The atmosphere is represented by a statistical-dynamical two-dimensional model (zonally averaged over ocean, land and sea-ice) with the resolution of 4° resolution and 11 vertical z-levels. Land, sea-ice and an active chemistry model are also included. The heat and moisture fluxes are provided by the two-dimensional atmosphere. Being zonally averaged, the longitudinal dependence of the fluxes is reconstructed through a "spreading" technique in which the total heat flux Q(y) is modified by adding the term dQ/dT*Δ(T(x,y)), and Δ(T) is the difference between the local temperature T(x,y) and the zonal mean. A flux correction term is applied to surface temperature and salinity by restoring them to the Levitus climatology through a nudging term.

The open boundary conditions of FVCOM for sea level, temperature and salinity, (u.v) at all levels are provided by the global MITgcm in both the coupled and uncoupled simulations. The surface heat fluxes for the ocean-only simulation are provided by the atmospheric component of the MITgcm. The wind stress however is given by the NCEP re-analysis with 6-hourly data. Four decade simulations (60s–70s–80s–90s) are available from the MITgcm with the full fields of currents, temperature, salinity and sea level. The complex spin-up procedure of the MITgcm can be found in http://mitgcm.org/public/r2_manual/latest/.

2.5 Coupling of RegCM3 and FVCOM

The OASIS3 software (http://www.cerfacs.fr/globc/software/oasis/oasis.html) is used to couple RegCM3 and FVCOM. It allows flexible coupling for different model configurations and is suitable to run on massively parallel computers. In order to keep synchronization of RegCM3 and FVCOM, the two models are integrated forward simultaneously and OASIS3 interpolates and transfers the coupling fields of different resolutions from the source grid to the target gird at a specified interval. RegCM3 and FVCOM are driven by the respective lateral boundary forcing. The coupling fields at the atmosphere–ocean interface are calculated in each model and exchanged through the coupler, that is, RegCM3 supplies the solar heat fluxes, latent and sensible heat flux, surface wind to FVCOM, and FVCOM provides SST to RegCM3. While at each time step the coupler is automatically requesting the coupling fields from the individual model, the exchange actually takes place every 6 h, the same frequency with which lateral boundary conditions are provided to RegCM3.

2.6 Model spin up for the coupled simulation

The first decade simulation (60 s) provided by the MITgcm is used for spin-up. The coupled model was first spun up from 1960 to 1969 for 10 years using the perpetual year of the decade of the 60 s, i.e. the weekly averages of surface forcings and variables prescribed at the open boundaries. A 10-year period is amply sufficient to spin up the wind-driven circulation, as demonstrated by monitoring the total kinetic energy of the basin (not shown) which stabilizes after ~3 years. For RegCM3, the SST is initialized with GISST data and then updated every 6 h using the SSTs obtained from FVCOM. FVCOM starts from rest with initial temperature and salinity from the first average January week of the 60 s. The temperature (salinity) at the boundaries is relaxed to the temperature (salinity) of the MITgcm simulation. Heat fluxes are updated every 6 h from RegCM3. To establish a realistic atmosphere–ocean interface thermal structure a flux correction is used during the model spin-up for the decade of the 60 s. Specifically, the SST is relaxed towards the SODA SST reanalysis (Carton et al. 2000a, b) with a depth dependent nudging factor, ranging from 0.2 s^{-1} in shallow water and decreasing to 0.001 s^{-1} in the open ocean. Thus in the open ocean the flux correction is negligible and the RegCM3 heat fluxes dominate. In shallow water the flux correction dominates to keep the ocean model from drifting from the climatology of the 60 s. Furthermore, to obtain a stable reversal monsoon circulation, sea level along the open boundaries at the Pacific and Indian Oceans is forced perpetually by 10-year averages of weekly SSHA simulation from the MITgcm, and the surface wind is gradually ramped up and updated every 6 h from RegCM3.

3 Results of the coupled model simulation

3.1 The ocean–atmosphere climatology from the coupled simulation

The simulation of the 70s was started from the model conditions saved at the end of the 60s. Differently from the spin-up phase and most importantly, no flux correction is used in the simulation of the 70s, hence in FVCOM relaxation of the SST to the observations is turned off. Secondly, the sea level at the open boundaries is driven by the real time sea level of the 70s, instead of using decadal averages as in the spin-up phase (60s).

We present only a few results from the coupled simulation to show that it reproduces realistically the well known south Asian monsoon seasonal cycle over the SCS, the Indonesian archipelago and the eastern Indian ocean. A detailed discussion of the atmospheric/oceanic properties of the region is well beyond the scope of the present work and can be found elsewhere (Aldrian et al. 2004, 2005; Gianotti et al. 2012; Gordon 2005; Gordon et al. 2010; Gan et al. 2006; Fang et al. 2009a, b; Xu and Malanotte-Rizzoli 2013).

Figure 3 shows the composite maps of the net heat flux for boreal Winter and Summer for the decade of the 70 s with superimposed the wind field from the coupled experiment, Fig. 3a, b, and the corresponding maps from the NCEP reanalysis, Fig. 3c, d. The modeled and observational fields are very similar showing the well known heat loss over the northwestern Pacific in Winter replaced by warming in Summer. The net heat flux patterns obviously reverse for the southern hemisphere. The Winter/Summer monsoon reversal is also well reproduced, northeastern in Winter and southwestern in Summer, even though the coupled winds are slightly stronger than the NCEP ones. Analogously, Fig. 4 shows the composite

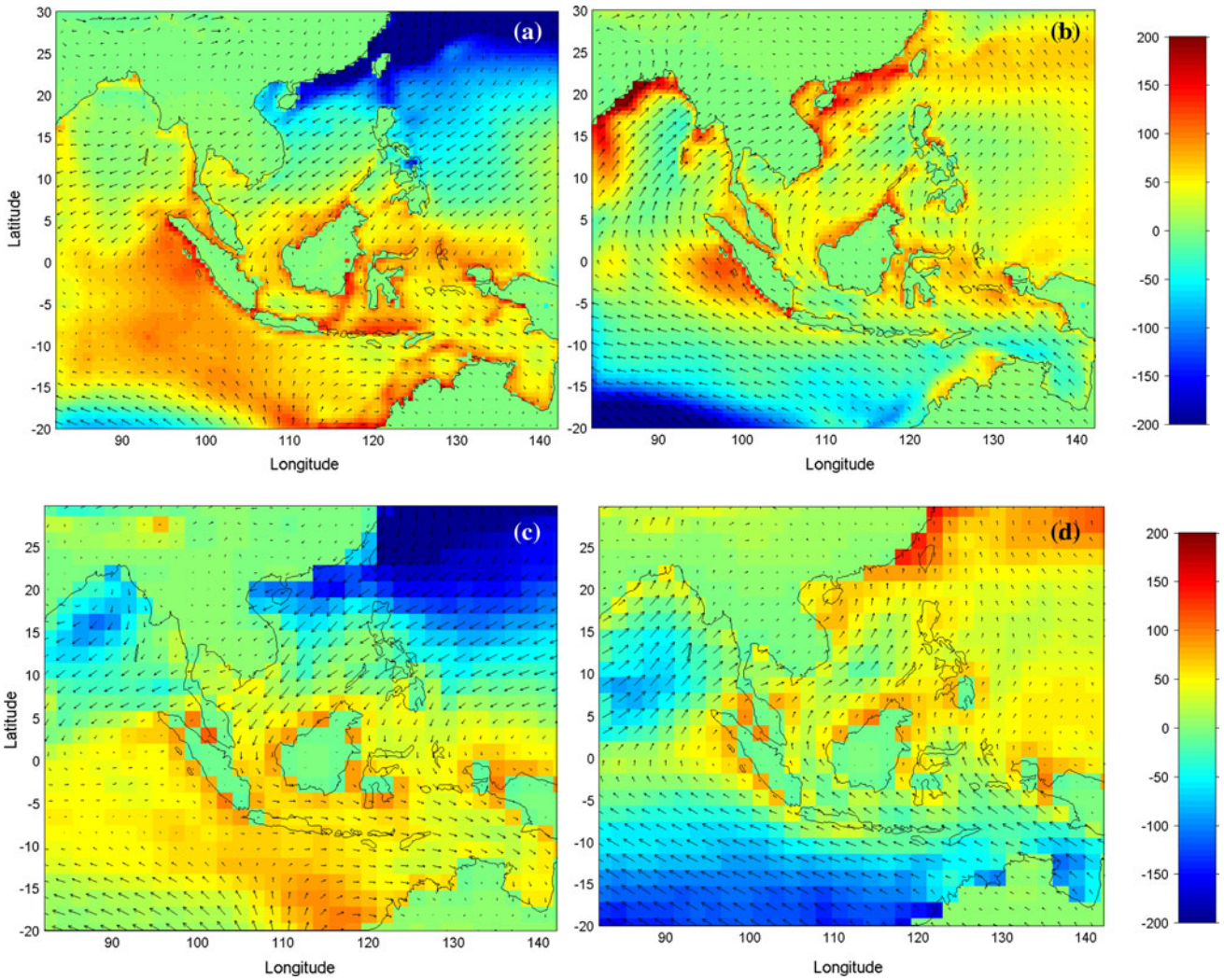

Fig. 3 Decadal average (1970s) coupled simulation of heat flux and winds for **a** winter and **b** summer. The wind vectors are shown every 100 km. NCEP heat fluxes and winds are shown in **c** winter and **d** summer for comparison

maps for the Winter/Summer ocean circulation with superimposed the SST from the coupled simulation, Fig. 4a, b, and the corresponding maps from the SODA reanalysis, Fig. 4c, d. The coupled experiment reproduces very well the seasonal reversal of the SCS through-flow associated with the reversal of the monsoon system, a result well known from the observational evidence and the modeling studies quoted above. The agreement with the SODA climatology is again very good, with the typical north/south progression of the SST matching the heat flux patterns of Fig. 3. The overall climatology of the Maritime Continent is therefore well simulated, even though our comparisons are necessarily only qualitative.

3.2 Comparison of the coupled with the atmosphere-only simulation and observations

We first carry out comparisons between the coupled and atmosphere-only simulation in which RegCM3 is forced as discussed in Sect. 2. Figure 5 shows the difference of the composite precipitation maps from the coupled simulation and the TRMM data for Winter, Fig. 5a, and Summer, Fig. 5b, respectively. Analogously, the difference between the RegCM3-only composite precipitation maps and the TRMM data are shown in Fig. 5c for Winter and Fig. 5d for Summer. The coupling is not very effective in reducing the errors in the precipitation fields. The range in precipitation

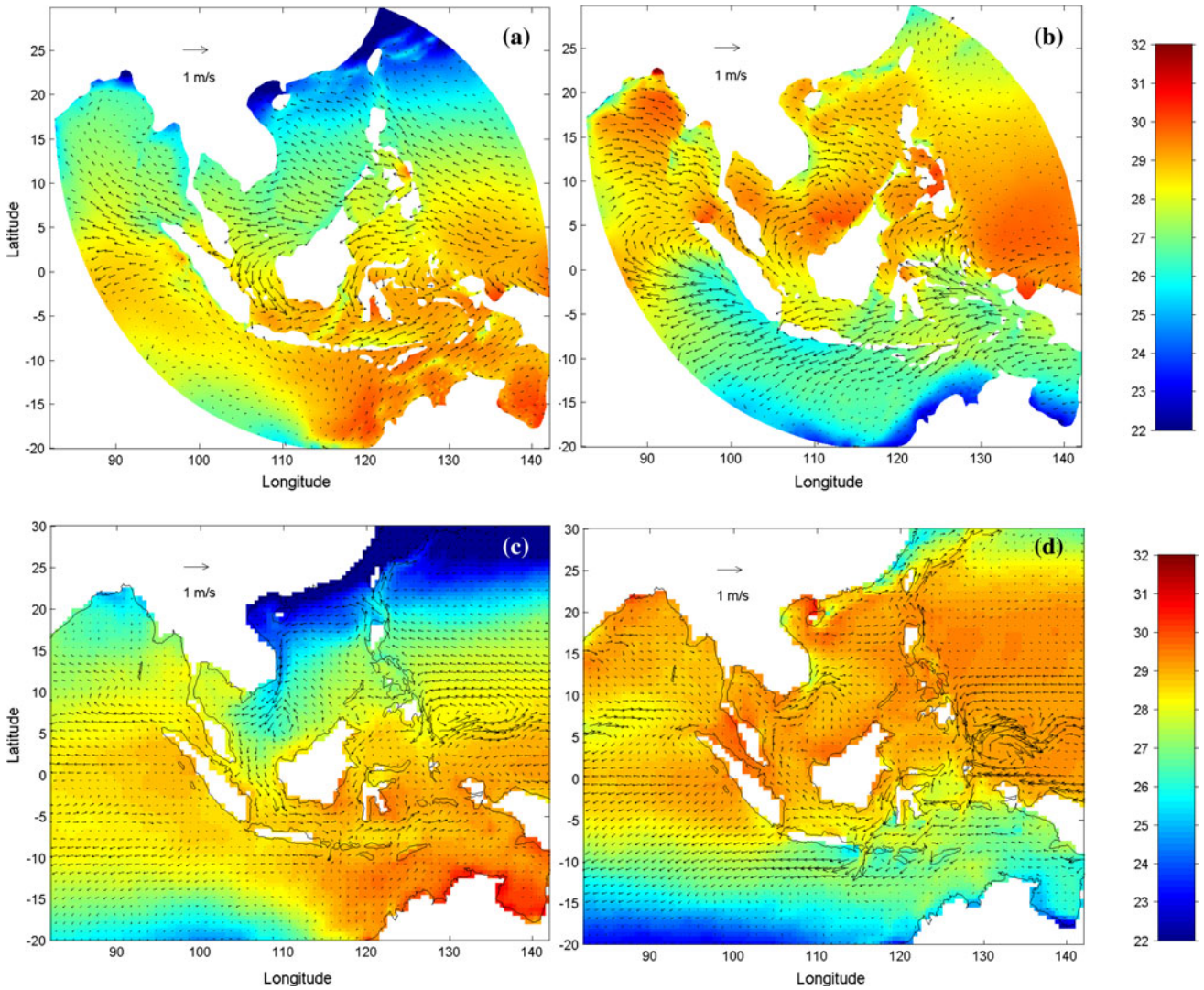

Fig. 4 Decadal average (1970s) coupled simulation of SST and surface currents for **a** winter and **b** summer. The vectors are given every 100 km. SODA SST and currents are shown in **c** winter and **d** summer for comparison

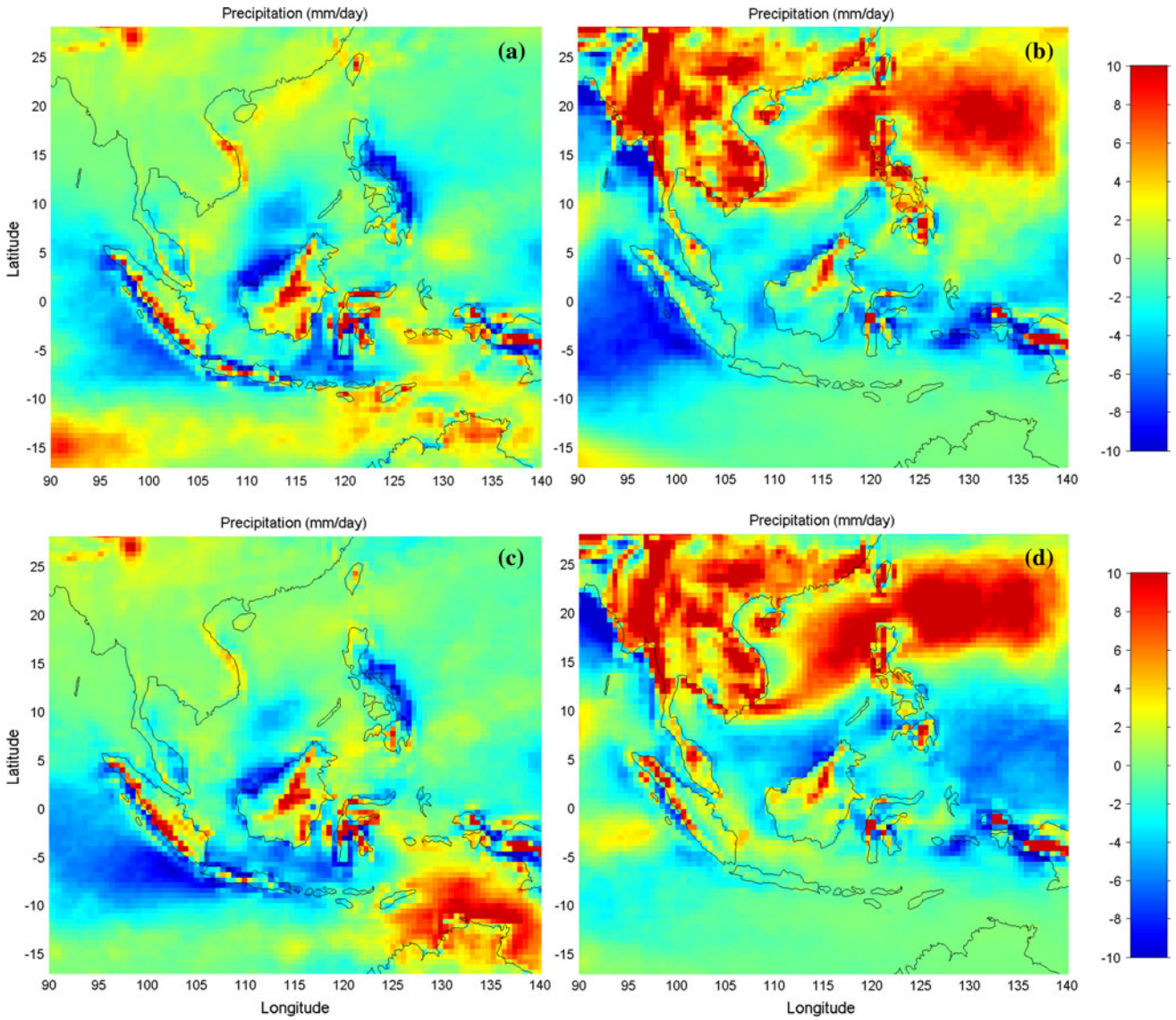

Fig. 5 Differences of the composite precipitation maps from the coupled simulation and TRMM observations for **a** winter and **b** summer, and from the RegCM3-only simulation and TRMM observations for **c** winter and **d** summer

errors is from −10 to +10 mm/day in both cases, and in both cases the error is positive reaching maximum values over land and negative reaching maximum values over the ocean. Closer examination of the difference maps shows however some improvement in the coupled simulation. In Winter, the regions of maximum negative as well maximum positive precipitation error are smaller in the coupled simulation, Fig. 5a, than in the RegCM3-only one, Fig. 5c. In Summer, the region of maximum positive error over land and the entire northern ocean of the coupled simulation, Fig. 5b, becomes even broader in the RegCM3-only one, Fig. 5d. The coupling may be less effective in improving the precipitation fields because precipitation is affected only indirectly by the ocean SST through feedbacks with atmospheric heat/moisture fluxes, as the two variables directly interacting with each other in the coupling are the SSTs and heat fluxes themselves.

To further assess the impact of coupling on precipitation, we carry out a comparison between the precipitation annual cycle from the coupled experiment and the TRMM data at three land stations located at different latitudes, Hong Kong at ∼23°N, Singapore at ∼2°N and Darwin and ∼13°S. The comparison is shown in Fig. 6. Simulated precipitation and observations are spatial averages within a box of 5° × 5° considering only the land points. Therefore the total points in the box for TRMM are 400 and 81 in RegCM3. The averages are carried out over land/total points as follows:

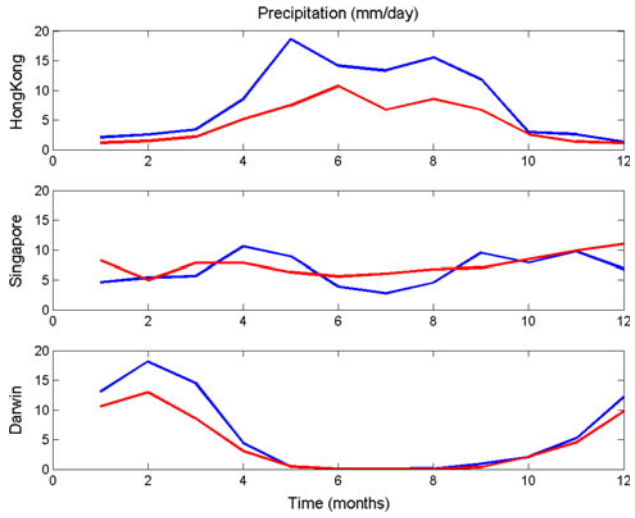

Fig. 6 Comparison of annual cycle between the coupled and observed (TRMM) precipitation at three locations: Hong Kong, Singapore and Darwin. The simulations and observations are spatial averages within a $5° \times 5°$ box centered at the three locations respectively

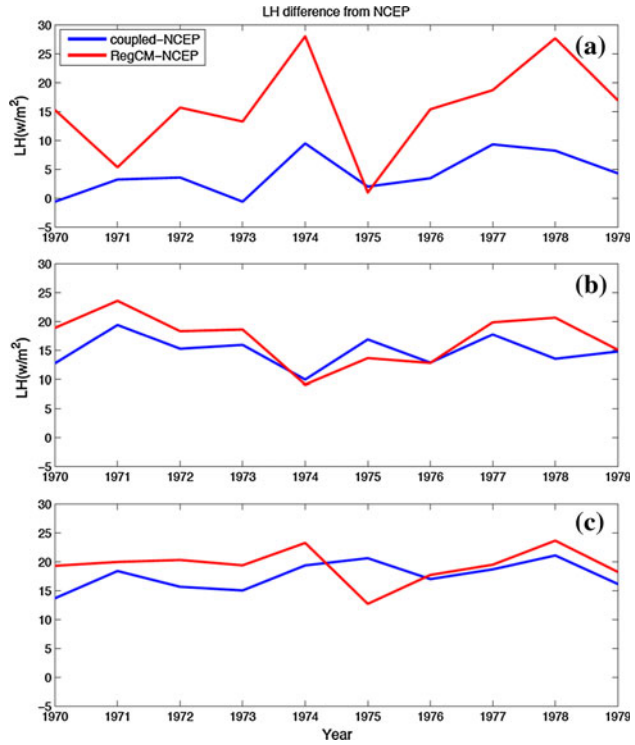

Fig. 7 The domain-averaged differences of latent heat flux between the coupled and NCEP reanalysis and differences between the RegCM3-only and NCEP reanalysis for **a** 10 successive summers, **b** 10 successive winters and **c** yearly averages

	Hong Kong	Singapore	Darwin
TRMM	196/400	180/400	179/400
Coupled model	42/81	35/81	34/81

The coupled simulation captures reasonably well the annual cycle of precipitation at Hong Kong and Darwin, with slightly less precipitation in the dry season and more in the wet one. At Singapore the simulated precipitation exhibits small variations around a mean consistent with the observed one. Overall, the coupled model seems to overestimate precipitation in Summer in the monsoon rain-belt (Hong Kong) and at lower latitudes in Winter (Darwin) with a maximum error of $\sim$10 mm/day at Hong Kong and $\sim$5 mm/day at Darwin.

As remarked above, the variables directly interacting with each other in the coupling are the ocean SST and the atmospheric heat flux. Among the heat flux components, the incoming solar radiation is externally imposed. The backscatter radiation and sensible heat are almost negligible. The heat component most affected by the SST is the latent heat, and we compare its evolution in the coupled and RegCM3-only simulation with the reference NCEP dataset. Specifically, Fig. 7 shows the domain-averaged difference between the coupled and NCEP latent heat for the 10 successive Summers of the 70 s (Fig. 7a); the 10 successive Winters (Fig. 7b); and the yearly averages (Fig. 7c), blue lines, as well the analogous differences between the RegCM3-only and the NCEP latent heat, red line. As evident from Fig. 7a, the Summer differences in the coupled latent heat (blue line) have an average of $\sim$5 Watts/m^2, much smaller than the $\sim$15 Watts/m^2 of the RegCM3-only latent heat (red line). 1975 was an anomalous year with a drop in latent heat even in the NCEP data. The 1975 anomaly is reflected in the Winter differences, Fig. 7b, where 1975 is the only year in which the coupled difference (blue line) is slightly worse than the RegCM3-only difference. The yearly difference, Fig. 7c, is obviously smoother, but the coupled model latent heat difference is consistently better (smaller) than the uncoupled one.

3.3 Comparison of the coupled with the ocean-only simulation and climatological observations

FVCOM is embedded in the MITgcm which provides the ocean variables at the open Pacific and Indian ocean boundaries. Consistently, in the ocean-only simulation FVCOM is forced at the surface by the meteorological variables used in the MITgcm global simulation, i.e. the NCEP winds and the heat fluxes evaluated by the zonally-averaged, two-dimensional atmospheric model as discussed in Sect. 2.4.

Figure 8 compares the time evolution over the decade of the 70s of atmospheric/oceanic properties from the coupled and ocean-only simulations as well as from the SODA climatology. Specifically, the left panels, Fig. 8a, c, show

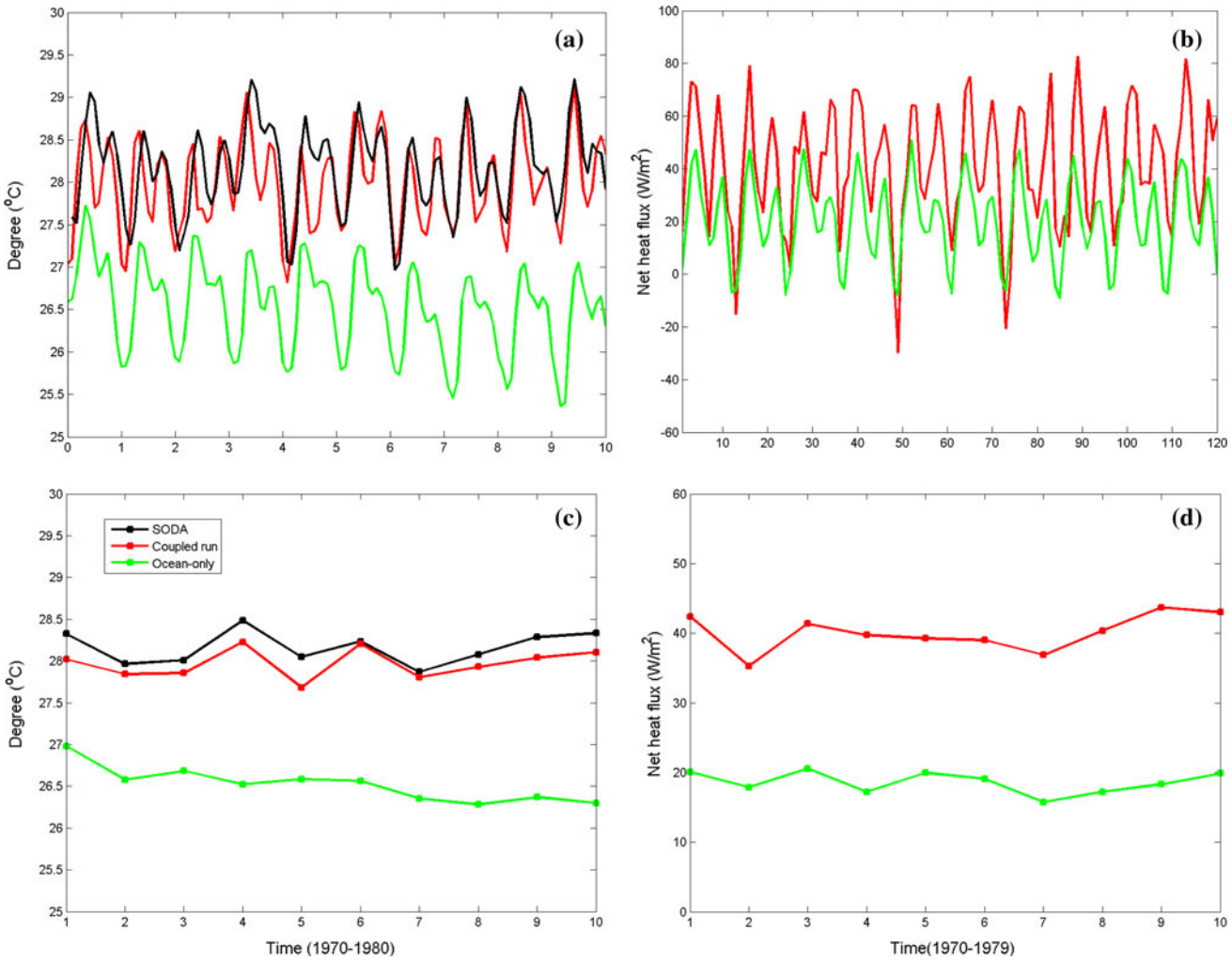

Fig. 8 Comparison of the coupled (*red lines*) and ocean-only (*green lines*) simulations. The *left panel* is **a** monthly and **c** yearly SST and the *right panel* is **b** monthly and **d** yearly net heat flux. SODA SST (*black lines*) is showed in **a**, **c** for comparison

the time evolution of the basin-averaged SST from the coupled model (red line), the ocean-only model (green line) and the SODA observations (black line) for the monthly averages, Fig. 8a, and yearly averages, Fig. 8c. The right panels show the analogous evolutions of the basin-averaged net heat flux from the coupled model (red line), the ocean-only model (green line) for the monthly averages, Fig. 8b, and yearly averages, Fig. 8d, respectively. The coupled SSTs reproduce fairly well the SODA climatology of the 70 s, red (coupled) and black (SODA) lines of Fig. 8a, c. The ocean-only SSTs on the other hand are underestimated by 1.5–2.2 °C. Also, the ocean-only SSTs exhibit a climate drift becoming progressively colder with $\sim$1.5 °C decrease over the 10-year period. The reduced SST amplitude of the ocean-only simulation is clearly due to the fact that the MITgcm net heat flux, green line in Fig. 8b, d, is $\sim$25 Watts/m^2 weaker than the coupled net heat flux, red line. The MITgcm net heat flux also shows a slight decreasing trend over the decade, albeit much smaller than the SST trend. Also, the SST cold drift is not caused by the model SST being out of phase with the observations. Figure 8a, c clearly show that the ocean-only SSTs, green line, are fully in phase with the SODA data, black line. A cross-correlation between the two evolutions (not presented) shows that the maximum correlation occurs at zero lag. Finally, examination of the difference between the ocean-only SSTs and the SODA data for the composite average Winter and Summer shows that the maximum errors, reaching ~ -9 °C, occur only over the southern South China Sea (Sunda shelf), the Gulf of Thailand and the Java Sea, all shallower than 50 m as shown by the 50 m isobaths in Fig. 2a. These differences are presented and discussed in the following Fig. 10.

To prove the hypothesis that these abnormal cold biases/drift in the ocean-only SSTs are due to the deficiency of the MITgcm heat fluxes, we carry out a further ocean-only

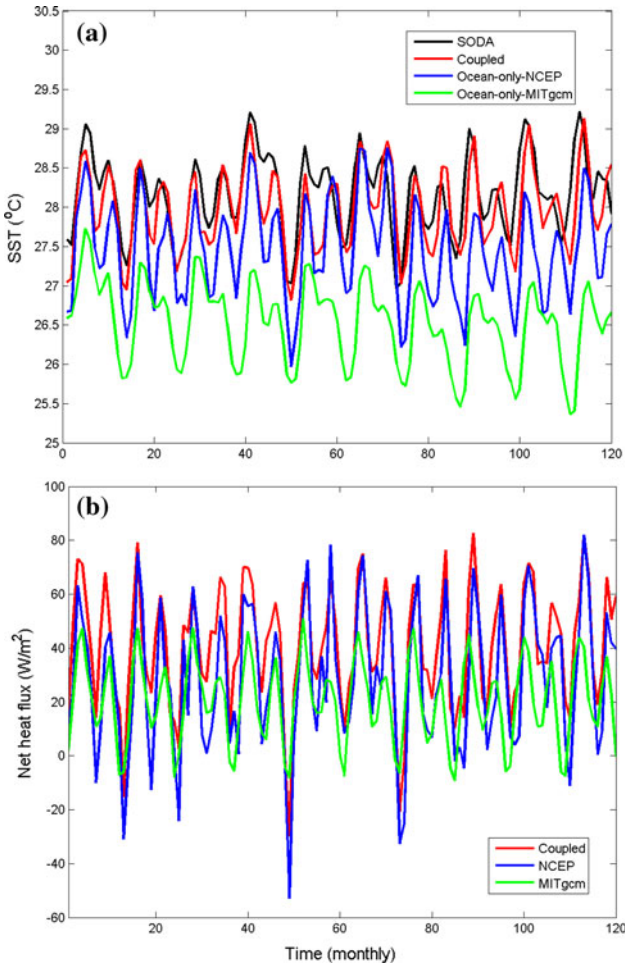

Fig. 9 Comparison of the monthly evolution of **a** SST from the coupled simulation (*red line*); the ocean-only simulation under NCEP heat fluxes (*blue line*); the ocean-only simulation under MITgcm fluxes (*green line*) and SODA data (*black line*); **b** coupled net heat flux (*red line*), NCEP net heat flux (*blue line*) and MITgcm net heat flux (*green line*)

simulation in which we force the ocean model with the NCEP heat fluxes. Figure 9a shows the monthly time evolution over the decade of the basin-averaged SSTs for the coupled simulation (red line); the ocean-only under NCEP fluxes (blue line); the ocean-only under MITgcm fluxes (green line); and the SODA observations (black line). The amplitude of the basin-averaged cold bias in the ocean-only simulation under NCEP fluxes is greatly reduced from ~ -2 to ~ -0.8 °C with respect to the coupled and SODA SSTs. Equally importantly, the cold drift in the SSTs is completely eliminated.

Figure 9b shows the monthly evolution over the decade of the coupled net heat flux (red line); the NCEP net heat flux (blue line); and the MITgcm net heat flux (green line). While the MITgcm heat flux is ~ 25 Watts/m^2 weaker than the coupled one, the NCEP heat flux is just ~ 10 Watts/m^2 weaker, explaining the corresponding reduced SST amplitudes. Also, the NCEP net heat flux does not exhibit any decreasing trend.

To examine closely the remarkable reduction of the cold biases under NCEP heat fluxes we zoom-in onto the region comprising the shallow seas where the cold biases are found. Figure 10 shows the difference between the ocean-only SSTs and SODA data for the composite average Winter and Summer. Specifically, the upper panel, Fig. 10a, b, shows the composite differences for the simulation under MITgcm heat fluxes. The middle panel, Fig 10c, d shows the differences for the simulation under NCEP heat fluxes. The maximum negative biases of -9 °C of the upper panel are drastically reduced to maximum biases of ~ -2 °C over much more limited areas and the cold, blue pools of Fig. 10a, b disappear in Fig. 10c, d. Finally, the lower panel, Fig. 10e, f, shows the same differences for the coupled simulation which basically eliminates the remaining biases of the ocean-only simulation as the temperature differences are in the range of observational errors.

In hindsight, the gross deficiency of the MITgcm heat fluxes is not surprising. They are evaluated by a zonally-averaged, two-dimensional atmosphere with an artificial reconstruction of the longitudinal dependence as discussed in Sect. 2.4. Furthermore, the very coarse resolution of 4° cannot resolve the small shallow seas embedded in the Indonesian archipelago. The residual bias in the ocean-only simulation under NCEP fluxes is obviously due to the still coarse resolution of the NCEP re-analysis and by the lack of feedback interactions between the atmospheric and ocean model components. The coupled simulation instead provides high resolution atmospheric heat fluxes which directly drive the ocean SST and are subsequently modified by them, thus correcting for the SST bias.

4 The ITF/SCS system

4.1 Oceanographic properties of the ITF/SCS system

We give a brief description of the oceanographic properties of the Maritime Continent which comprises the South China Sea (SCS) and its through-flow (SCSTF) and the Indonesian Through-Flow (ITF). The latter one constitutes the major conduit of tropical waters from the western Pacific to the eastern Indian ocean and comprises multiple pathways through the straits of the Indonesian archipelago. All the straits containing pathways of the SCSTF and ITF are marked in Fig. 2b.

The SCS connects the subtropical western Pacific to the southern Java sea (Fig. 2a). Surface heat and moisture fluxes are especially important for the SCS which gains

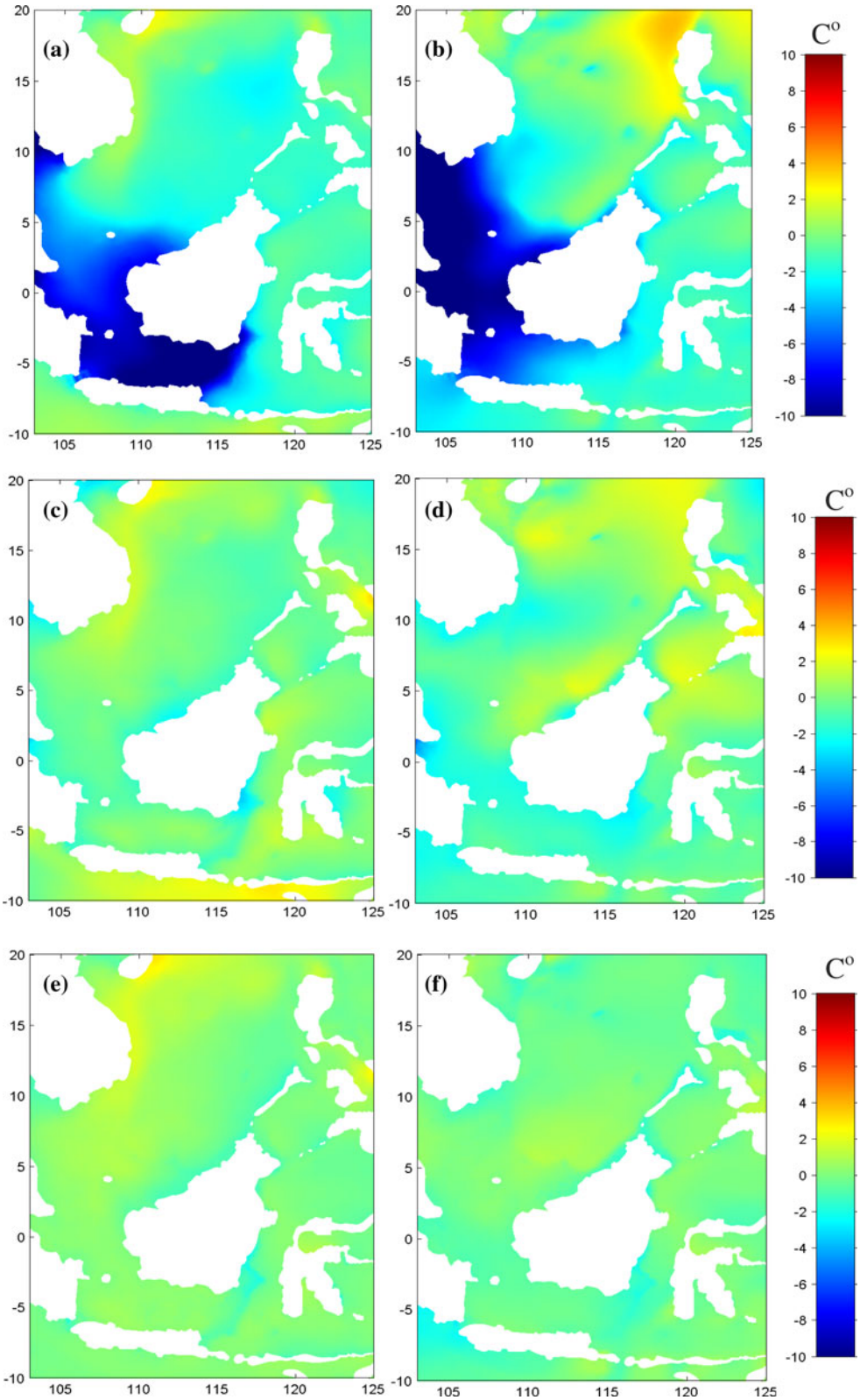

Fig. 10 Decadal-average SST difference with SODA for ocean-only simulation under MITgcm heat fluxes in winter **a** and summer **b**; ocean-only simulation under NCEP fluxes in winter **c** and summer **d**; and coupled in winter **e** and summer **f**

heat from the atmosphere at a rate of ~20–50 Watts/m^2 per year and is a recipient of heavy rainfall with an annual mean value of ~0.2–0.3 Sv (1 Sv = 10^6 m^3/sec) over the entire basin. On the long time average, the heat and freshwater gain are balanced by horizontal advection by the mean circulation. The SCSTF originates in the northern,

Table 1 Annual averaged volume transport (Sv) of ITF outflow (Negative is westward/southward)

	ITF outflow		
	Lombok	Ombai	Timor
60 s	−3.7	−6.7	−6.4
90 s	−3.8	−7.3	−7.8
70 s	−3.7	−7.2	−7.4
70 s coupled	−4.1	−8.6	−10.5
INSTANT	−2.6	−4.9	−7.5
INSTANT uncertainties	−1.8 to −3.2	−2.7 to −5	−6.2 to −10.5

Table 2 Annual averaged volume transport (Sv) of Makassar Strait (Negative is southward)

	ITF inflow Makassar
60s	−9.6
90s	−10.3
70s	−10.4
70s coupled	−11.7
INSTANT	−11.6
INSTANT uncertainties	−8.3 to −14.9

deep Luzon strait through which the cold, salty water of the western subtropical Pacific enters into the SCS. Through the air–sea fluxes, this water is transformed into warm, fresh water exiting from the Mindoro strait and the southern shallow Karimata strait into the Java sea, the terminal point of the SCSTF. For a review of the SCS/SCSTF properties see Qu et al. (2009).

In the ITF the transfer of tropical western Pacific waters is closely linked by air-sea fluxes to coupled modes of climate variability, such as El Nino/Southern Oscillation (ENSO), the Asian Monsoon and the Indian Ocean Dipole (IOD) (Gordon 2005; Gordon et al. 2012). The ITF comprises multiple pathways, but the Makassar strait is the primary inflow passage for the Pacific waters carrying ∼80 % of the total ITF transport. For a review of the ITF properties see Gordon (2005) and Gordon et al. (2010). The ITF outflow pathways are the Lombok, Ombai and Timor straits, all marked in Fig. 2b. The importance of the ITF for the tropical climate has been long recognized and major observational programs, described in the next section, were first established in the late 90 s. In contrast, no systematic observational effort has yet been conducted for the SCSTF, even though recently its importance for the volume and heat exchanges among the various Indonesian seas has been recognized. In the modeling study of Xu and Malanotte-Rizzoli (2013) the SCSTF has been shown to affect crucially the ITF, opposing and even reversing it in

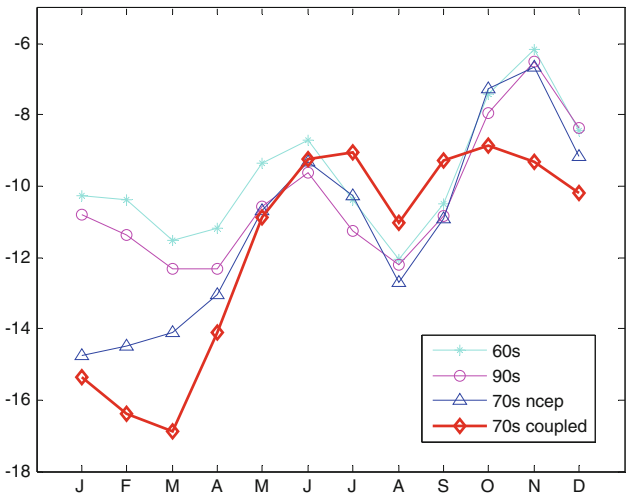

Fig. 11 Yearly cycle of the Makassar transport for all the simulations, ocean-only (60s, 90s and 70s ncep) and coupled (70s)

the surface layer during Winter. Gordon et al. (2012) also show that increased SCSTF during the El Nino event of 2008-09, with the corresponding increase of the southward flow through the Sulu sea into the Makassar strait, prevents the injection of tropical Pacific surface water into the strait itself. Oppositely, during La Nina the SCSTF is negligible allowing tropical Pacific inflow.

This increasing evidence of the crucial importance of the SCSTF/ITF interactions for the Pacific/Indian ocean connections clearly indicates that only regional climate models whose coupled domain covers the entire Indonesian Maritime Continent can capture the coupled ocean–atmosphere tropical modes of interannual and decadal climate variability.

4.2 Comparisons of ocean-only and coupled simulations with ITF observations

For the comparisons here discussed we use exclusively the ocean-only simulations under NCEP heat fluxes in which the basin-average cold bias is reduced to ∼−0.8 °C with a maximum values of −2 °C in the southern shallow SCS. As previously remarked, Xu and Malanotte-Rizzoli (2013) investigates the climatologies of the two decades 60s and 90s in ocean-only simulation comparing properties of the wind-driven circulation and differences in the thermal structure of the SCS induced by the observed global ocean warming between the two decades (Levitus et al. 2000, 2005). Here we have focused on the climatology of the 70s which belongs to the pre-warming phase. The major difference between the ocean-only simulations of Xu and Malanotte-Rizzoli (2013) and the present ones is that they relaxed the SSTs towards the SODA re-analysis data while here we do not and use only the surface forcing provided by the NCEP heat fluxes.

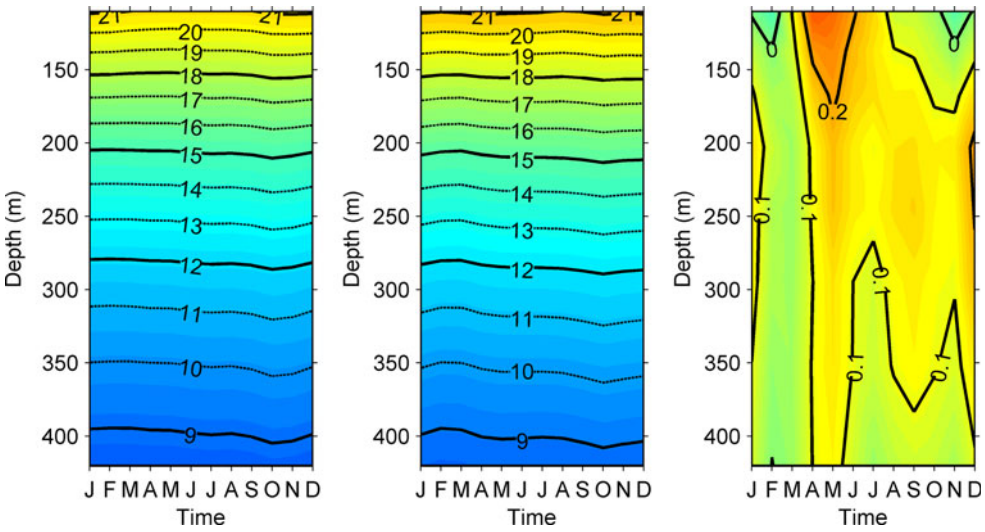

Fig. 12 Mean seasonal temperature section across the Makassar strait: seasonal section for the decadal climatology of the 70s from the ocean-only (*left panel*), coupled simulations (*middle panel*) and their difference (*right panel*). Units are °C

As previously remarked, no systematic observational programs have yet been established for the SCS/SCSTF. Estimates of the northern Luzon transport are a combination of sparse observations and modeling results and are summarized by Fang et al. (2009a, b) and Xu and Malanotte-Rizzoli (2013). No measurements existed for the Karimata strait until the recent observations by Fang et al. (2010) which however cover only the boreal Winter 2007–2008. In contrast, the ITF has been the object of a first observational effort during the 1996-1998 ARLINDO program (Gordon and McClean 1999) followed by the later intensive International Nusantara Stratification and Transport (INSTANT) program which covered the three years 2004–2006. (Sprintall et al. 2009; Gordon et al. 2010). The INSTANT program was established to simultaneously measure the ITF from the Pacific inflow at the Makassar strait and Lifamatola Passage to the Indian ocean exit straits of Timor, Ombai and Lombak. During INSTANT two moorings were deployed inside the Makassar strait. When INSTANT ended in 2006, a single mooring was redeployed until May 2009, providing nearly 5.5 years of observations inside the strait. Because of this intensive observational effort for the ITF, we focus on comparing our simulation results with the INSTANT measurements as well as with the previous transport estimates provided by Xu and Malanotte-Rizzoli (2013).

Table 1 provides the annual average transport estimates of the ITF outflow through the Lombok, Ombai and Timor straits for the 60 s and 90 s (from Xu and Malanotte-Rizzoli 2013), the 70 s, our ocean-only and coupled simulations, the INSTANT observational values and their uncertainties (Sprintall et al. 2009). We do not report the estimates for the Lifamatola strait as the INSTANT observations extend only from 1,250 m to the bottom.

The estimates of the Lombok and Ombai transports are all greater than the observational values and in the same range, while for Timor all of them fall inside the uncertainty range. No statement can be made about which estimate is better.

The situation is very different for the Makassar strait where the INSTANT observations are the longest and most extensively analyzed. Table 2 provides the estimates of the mean Makassar transports for the three ocean-only, the coupled simulation and INSTANT. The coupled transport estimate is the absolute best, almost coinciding with the INSTANT value, while the ocean-only values are all under-estimated.

Figure 11 shows the yearly cycle of the Makassar transport for all the simulations to be compared with the INSTANT observed cycle for 2005 shown in Gordon et al. (2008), their Fig. 3, negative values indicating southward transport. As reported in Susanto et al. (2012), during the 2004-2006 INSTANT period the ENSO phase was in a relatively neutral state, especially in 2005, with a weak El Nino at the end of 2004 and a weak La Nina at the beginning of 2006 (Susanto et al. 2012, their Fig. 9). Therefore 2005 is the year most comparable to our climatologies. The seasonal cycle of the Makassar transport is well reproduced in all the simulations, with the observed southward maxima occurring in March and August and minima in June and October/November. The coupled simulation overestimates the November minimum which is better reproduced by the ocean-only simulations. On the other hand, the coupled simulation is the only one fully capturing the maximum INSTANT transport in March both in amplitude and phase. Combined with the yearly cycle, the yearly average transport estimate given in Table 2 clearly shows that the coupled simulation is the overall best.

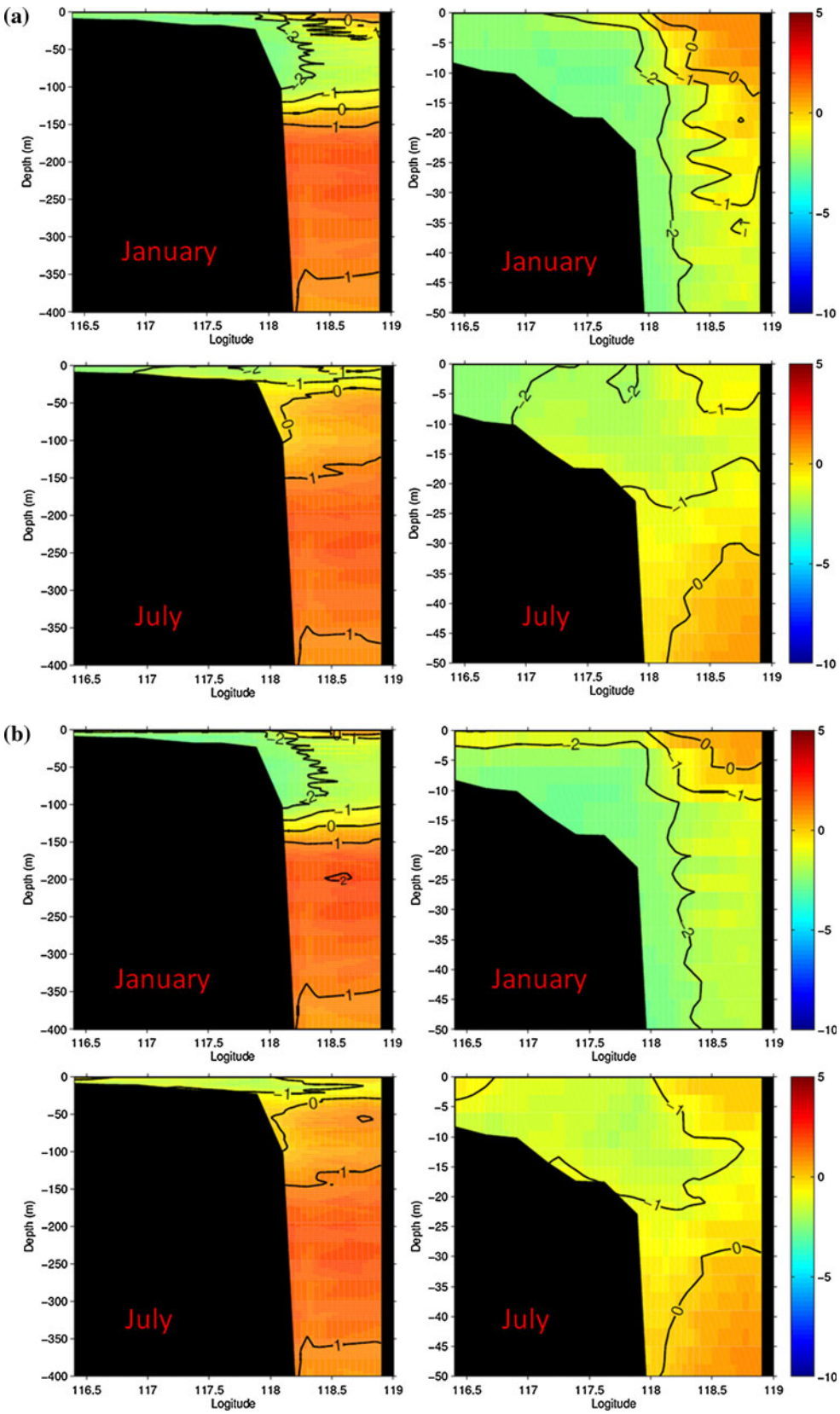

Fig. 13 **a** Differences in °C in the vertical temperature section though the Makassar strait between the ocean-only simulation under NCEP fluxes and the SODA re-analysis for the 70s. **b** as in **a** but for the coupled simulation

To further assess the performance of the ocean-only and coupled simulations and to better understand the implications of coupling for air–sea fluxes, we analyze the vertical thermal structure of the Makassar cross-section analyzed in INSTANT. For it, Susanto et al. (2012) constructed the mean seasonal temperature section for the INSTANT years 2004–2006, their Fig. 6. Figure 12 shows the analogous seasonal sections for the 70s from the ocean-only simulation, left panel, and the coupled one, middle panel, respectively. The overall thermal structure of the section is well reconstructed in both simulations with all the temperature isolines in the correct depth ranges. The modeled thermoclines are smoother representing a decadal climatology and the comparison can be only qualitative. The right panel of Fig. 12 gives the temperature differences between the coupled and ocean-only simulations. The coupled thermocline in the interior of the Makassar strait is 0.1–0.2 °C warmer than the ocean-only one under the NCEP fluxes. This is consistent with the negative SST bias under the NCEP fluxes which is eliminated by the coupling resulting in a warmer thermocline especially in the surface layer.

We obtain a quantitative assessment of the performance of the coupled and ocean-only simulations by using the SODA re-analysis of the 70s for the comparison. In fact, Tillinger and Gordon (2010) showed that the SODA temperature data within the Labani channel in the center of the Makassar strait approximate extremely closely the mean vertical temperature profile of both the ARLINDO and INSTANT experiments, see their Fig. 2. Figure 13a, b show the differences in the vertical temperature section across Makassar between the ocean-only simulation under NCEP fluxes and SODA, Fig. 13a, and the coupled one and SODA, Fig. 13b. Specifically the upper panels give the section differences for January and the lower ones for July; the left panels reach the depth of 400 m and the right ones zoom-in the surface 50 m layer.

As evident from Fig. 13a, b there is no difference between the ocean-only and coupled thermal stratifications below the upper layer of 50 m. This is a foregone result as the effects of air–sea heat fluxes remains confined to the surface layer. An increased surface net heat flux, such as the one observed in the 90 s over the SCS, does not diffuse heat below $\sim$50 m depth (Xu and Malanotte-Rizzoli 2013). Differences between the two simulations emerge in the surface layer, right panels of Fig. 13a, b. In January the water mass over the entire Makassar shelf in the ocean-only result, Fig. 13a upper right panel, is colder than SODA by ~ -2 °C. The deeper part of the strait also shows a pool of water ~ -1 °C colder than SODA down to $\sim$30 m depth. At the surface, in the right corner, the water is warmer than SODA by $\sim$1.5 °C. In the January coupled simulation, on the other hand, Fig. 13b upper right panel, the pool of colder water mass on the shelf is smaller and is capped by a thin layer of water only ~ -0.5 °C colder than SODA. The pool of colder water on the right side of the strait is also much smaller, penetrating only to 10 m depth, and in the right upper corner only a very small pool remains warmer than +0.5 °C. In July, in the ocean-only result, Fig. 13a lower right panel, again the Makassar shelf is covered by a water mass ~ -2 °C colder than SODA and the remainder of the upper $\sim$25 m of the strait shows water ~ -1 °C colder. In the coupled simulation, Fig. 13b lower right panel, only a rather smaller pool of colder water is present on the shelf, while the remainder of the section has basically zero temperature difference from SODA. These temperature sections clearly show that the upper thermocline structure of the Makassar strait is considerably better in the coupled simulation.

5 Conclusions

Simulations of the climate of the Maritime Continent have been carried out focusing on decadal climatologies. The coupled climate model consists of a regional atmospheric model, RegCM3, and a regional ocean model, FVCOM. The coupled domain coincides with the ocean model domain and comprises all the conduits from the western Pacific tropical and subtropical interior to the eastern Indian ocean through the straits of the ITF and SCSTF. The coupled domain can therefore capture the transmission from the Pacific to the Indian ocean of coupled climate modes with interannual and decadal variability such as ENSO.

For RegCM3, boundary forcing is provided by the ECMWF-ERA40 re-analysis at 6 h frequency. FVCOM is embedded in the global MITgcm which provides the boundary forcing to the regional FVCOM. Four decades of weekly averages of all atmospheric and oceanic dynamic variables are available from the MITgcm for the period 1960–2000. The two decades 1960–69 and 1990–99 have been investigated in ocean-only simulations by Xu and Malanotte-Rizzoli (2013). Here we extend the investigation to the decade 1970-79 with both ocean-only and coupled simulations. Their results are compared and analyzed against available observations.

For the atmospheric component, the analysis focuses on precipitation climatology, i.e. seasonal composite maps and annual precipitation cycle at specific land stations, and on the domain-averaged monthly and yearly cycles of latent heat and net heat flux for the decade. Both coupled and atmosphere-only flux evolutions are assessed against the NCEP re-analysis. For the oceanic component the focus is first on the domain-averaged SST evolution over the decade in the coupled model and under two different air-sea

flux forcing for the uncoupled simulations. Both uncoupled and coupled SST evolutions are assessed against the SODA re-analysis. Successively, a detailed analysis is carried out on the oceanic circulation properties of the ITF. The transport yearly cycles through the Makassar strait, which carries $\sim$80 % of the total ITF transport, are compared for the three decades 60s–70s–90s of ocean-only simulations with the coupled 70s simulation and the INSTANT observations. For the thermal structure of the Makassar strait cross-section the coupled and uncoupled results for the 70s are compared with the INSTANT temperature section and the SODA re-analysis.

The coupled model is able to produce stable and realistic decadal evolution of atmospheric/oceanic variables without flux correction. Furthermore, in most cases the coupled results are better than the uncoupled one.

Specifically, for precipitation the comparison with TRMM data at three land stations at different latitudes shows that the coupled simulation captures the annual cycle rather well. On the other hand, the coupling is not very effective in reducing the errors in the composite seasonal precipitation fields when compared with the atmospheric-only results, even though some improvements can be detected in the coupled difference maps. Precipitation however is affected only indirectly by the ocean SST through feedbacks with atmospheric heat/moisture fluxes. The variables directly interacting with each other in the coupling are the ocean SST and the atmospheric latent heat flux. The domain-averaged difference between the modeled and NCEP latent heat flux for the Winter, Summer and yearly evolutions over the decade shows that the coupled latent heat flux is consistently better than the uncoupled one.

For the oceanic SST, ocean-only simulations are carried out under two different heat flux forcing. As the ocean model is embedded in the global MITgcm, an ocean-only simulation was first carried out using the MITgcm heat fluxes. The simulation produced a grossly deficient monthly evolution of the basin-averaged SST with an average cold bias of ~ -2 °C and a cold drift of ~ -1.5 °C over the decade. A second ocean-only evolution forced by the NCEP heat fluxes reduced the average cold bias to ~ -0.8 °C and eliminated the drift. Extreme cold SST anomalies over the shallow enclosed seas of the ITF produced by the MITgcm fluxes were drastically reduced under the NCEP ones and disappeared in the coupled simulation. The latter one produces a fully realistic SST evolution when compared with the SODA re-analysis. The gross deficiency of the MITgcm heat fluxes is due to the fact that they are evaluated by a zonally-averaged two-dimensional atmosphere with the very coarse resolution of 4° which cannot resolve the small shallow seas of the Indonesian archipelago. Hence only the NCEP fluxes were subsequently used in the ocean-only simulations.

The detailed oceanographic comparisons of the simulations with the INSTANT observations show that the coupled simulation produces the best total transport estimate for the Makassar strait, while the ocean-only average transports for the 60s–70s–90s are all significantly underestimated. The yearly transport cycle is also well reproduced when assessed against INSTANT. Both the coupled and uncoupled simulations reconstruct a realistic seasonal thermal structure of the Makassar cross-section when compared with the INSTANT one. The comparison however is only qualitative. To obtain a quantitative assessment of the two simulations, we compare them with the SODA re-analysis for Winter and Summer. The comparison shows that the coupling considerably improves the vertical thermal structure of the section in the upper layer affected by the surface heat fluxes.

In summary, the coupling has overall positive implications both for the atmosphere and the ocean. In particular coupling produces a considerable improvement in the climatological monthly evolution of the SST assessed against the SODA data and in the ocean circulation assessed against the INSTANT observations in the Makassar strait. The latter one is the major conduit of the ITF which transfers water properties from the western Pacific to the Indian ocean closely linked by air-sea fluxes to coupled modes of climate variability such as ENSO. We believe that the improvement produced by coupling in the ocean circulation is due to the fact that our coupled domain captures all these transfers. On the other hand, the relative ineffectiveness of the coupling on the precipitation fields requires a closer examination of the atmosphere–ocean feedbacks between SST and atmospheric heat fluxes and the latter effects on precipitation.

Acknowledgments This study was supported by the Singapore National Research Foundation (NRF) through Center for Environmental Sensing and Monitoring (CENSAM) under the Singapore-MIT Alliance for Research and Technology (SMART) program and by National Natural Science Foundation of China (NSFC, No. 41106003).

References

Aldrian E, Jacob D, Podzun R, Gates LD, Gunawan D (2004) Long term simulation of the Indonesian rainfall with the MPI regional model. Clim Dyn 22:795–814

Aldrian E, Sein D, Jacob D, Dümenil Gates L, Podzun R (2005) Modeling Indonesian rainfall with a coupled regional model. Clim Dyn 25:1–17

Carton JA, Chepurin G, Cao X, Giese BS (2000a) A simple ocean data assimilation analysis of the global upper ocean 1950–1995, Part 1: methodology. J Phys Oceanogr 30:294–309

Carton JA, Chepurin G, Cao X (2000b) A simple ocean data assimilation analysis of the global upper ocean 1950–1995 Part 2: results. J Phys Oceanogr 30:311–326

Chen C, Liu H, Beardsley RC (2003) An unstructured, finite-volume, three-dimensional, primitive equation ocean model: application to coastal ocean and estuaries. J Atmos Oceanic Tech 20:159–186

Chen C, Beardsley RC, Cowles G (2006a) An unstructured grid, finite-volume coastal ocean model-FVCOM user manual, School for Marine Science and Technology, University of Massachusetts Dartmouth, New Bedford, Second Edition. Technical Report SMAST/UMASSD-06-0602, p. 318

Chen C, Beardsley RC, Cowles G (2006b) An unstructured grid, finite-volume coastal ocean model (FVCOM) system. Special issue entitled "advance in computational oceanography". Oceanography 19(1):78–89

Fang G, Wang Y, Wei Z, Fang Y, Qiao F, Hu X (2009a) Interocean circulation and heat and freshwater budgets of the South China Sea based on a numerical model. Dyn Atmos Oceans 47:55–72

Fang Y, Zhang Y, Tang J, Ren X (2009b) A regional air-sea coupled model and its application over East Asia in the summer of 2000. Adv Atmos Sci. doi:10.1007/s00376-009-8203-7

Fang G, Susanto RD, Wirasantosa S, Qiao F, Supangat A, Fan B, Wei Z, Sulistiyo B, Li S (2010) Volume, heat and freshwater transports form the South China Sea to Indonesian seas in the boreal winter of 2007–2008. J Geophys Res 115:C12020. doi:10.1029/2010JC006225

Gan J, Li H, Curchitser EN, Haidvogel DB (2006) Modeling South China Sea Circulation: response to seasonal forcing regimes. J Geophys Res 111:C06034. doi:10.1029/2005JC003298

Gianotti RL, Zhang D, Eltahir EAB (2012) Assessment of the regional climate model version 3 over the maritime continent using different cumulus parameterization and land surface schemes. J Climate 25:638–656. doi:10.1175/JCLI-D-11-00025.1

Giorgi F, Marinucci MR, Bates GT (1993) Development of a second-generation regional climate model (RegCM2). Part I: boundary-layer and radiative transfer processes. Mon Wea Rev 121:2794–2813

Gordon AL (2005) Oceanography of the Indonesian seas and their through-flow. Oceanography 18(4):14–27

Gordon AL, McClean JL (1999) Thermohaline stratification of the Indonesian Seas: model and observations. J Phys Oceanogr 29:198–216

Gordon AL, Susanto RD, Ffield A, Huber BA, Pranowo W, Wirasantosa S (2008) Makassar Strait throughflow, 2004 to 2006. Geophys Res Lett 35:L24605. doi:10.1029/2008GL036372

Gordon AL, Sprintall J, Van Aken HM, Susanto D, Wijffels S, Molcard R, Ffield A, Pranowo W, Wirasantosa S (2010) The Indonesian throughflow during 2004–2006 as observed by the INSTANT program. Dyn Atmos Oceans 50:115–128. doi:10.1016/j.dynatmoce.2009.12.002

Gordon AL, Huber BA, Metzger EJ, Susanto RD, Hurlburt HE, Adi TR (2012) South China Sea throughflow impact on the Indonesian throughflow. Geophys Res Lett 39:L11602. doi:10.1029/2012GL052021

Grell GA, Dudhia J, Stauffer DR (1994) Description of the fifth generation Penn State/NCAR Mesoscale Model (MM5), Technical Report TN-398 + STR. National Center for Atmospheric Research, Boulder

Gualdi S, Somot S, Li L, Artale V, Adani M, Bellucci A, Braun A, Calmanti S, Carillo A, Dell'Aquilla A, Déqué M, Dubois C, Elizalde A, Harzallah A, Jacob D, Lheveder B, May W, Oddo P, Ruti P, Sanna A, Sannino G, Sevault F, Scoccimarro E, Navarra A (2012) The CIRCE simulations: a new set of regional climate change projections performed with a realistic representation of the Mediterranean Sea. Bull Amer Meteor Soc. doi:10.1175/BAMS-D-11-00136.1

Hill C, Marshall J (1995) Application of a parallel Navier-Stokes model to ocean circulation in parallel computational fluid dynamics In: Proceedings of parallel computational fluid dynamics: implementations and results using parallel computers, pp 545–552

Holtslag AAM, de Bruijn EIF, Pan H-L (1990) A high-resolution air mass transformation model for short-range weather forecasting. Mon Wea Rev 118:1561–1575

Huffman GJ, Adler RF, Bolvin DT, Gu G, Nelkin EJ, Bowman KP, Hong Y, Stocker EF, Wolff DB (2007) The TRMM multi-satellite precipitation analysis: quasi-global, multi-year, combined-sensor precipitation estimates at fine scale. J Hydrometeor 8:38–55

Kalnay E, Kanamitsu M et al (1996) The NCEP/NCAR 40-year Reanalysis Project. Bull Amer Meteor Soc 77:437–471

Kiehl JT, Hack JJ, Bonan GB, Boville BA, Breigleb BP, Williamson DL, Rasch PJ (1996) Description of the NCAR Community Climate Model (CCM3), NCAR Technical Note TN-420 + STR, [Available online at: http://www.cgd.ucar.edu/cms/ccm3/TN-420/]

Levitus S, Antonov JI, Boyer TP, Stephens C (2000) Warming the world ocean. Science 287:2225–2229

Levitus S, Antonov JI, Boyer TP (2005) Warming of the World Ocean, 1955-2003. Geophys Res Lett 32:L02604. doi:10.1029GL021592

Li T, Zhou GQ (2010) Preliminary results of a regional air-sea coupled model over East Asia. Chinese Sci Bull 55:2295. doi:10.1007/s11434-010-0071-0

Marshall J, Hill C, Perelman L, Adcroft A (1997) Hydrostatic, quasi-hydrostatic, and nonhydrostatic ocean modeling. J Geophys Res 102(C3): 5733–5752

Mellor GL, Yamada T (1982) Development of a turbulence closure model for geophysical fluid problem. Rev Geophys Space Phys 20:851–875

Pal JS et al (2007) Regional climate modeling for the developing world: the ICTP RegCM3 and RegCNET. Bull Am Meteorol Soc 88:1395–1409

Qu T, Song YT, Yamagata T (2009) An introduction to the South China Sea through-floe: its dynamics, variability and application for climate. Dyn Atnos Oceans 47:3–14

Rayner NA, Horton EB, Parker DE, Folland CK, Hackett RB (1996) Version 2.2 of the global sea-ice and sea-surface temperature data set, 1903–1994. Technical Note CRTN74. Clim Res p 35

Ren X, Qian Y (2005) A coupled regional air–sea model, its performances and climate drift in simulation of the east Asian summer monsoon in 1998. Int J Climatol 25:679–692

Smagorinsky J (1963) General circulation experiments with the primitive equations, I. The basic experi-ment. Mon Wea Rev 91:99–164

Sprintall J, Wijffels S, Molcard R, Jaya I (2009) Direct estimates of the Indonesian throughflow entering the Indian Ocean: 2004-2006. J Geophys Res 114:C7. doi:10.1029/2008JC005257

Susanto RD, Ffield A, Gordon AL, Adi TR (2012) Variability of Indonesian throughflow within Makassar Strait, 2004–2009. J Geophys Res 117:C0913. doi:10.1029/2012JC008096

Terray L, Valcke S, Piacentini A, 1999: OASIS 2.3 Ocean atmosphere sea ice soil user's guide. Technical Report TR/CGMC/99-37 CERFACS p 82

Tillinger D, Gordon AL (2010) Transport weighted temperature and internal energy transport of the Indonesian throughflow. Dyn Atmos Oceans 50:224–232

Uppala SM et al. (2005) The ERA-40 Re-Analysis. Q J R Meteorol Soc 131:2961–3012. [Dataset available online at: http://www.ecmwf.int/research/era/do/get/era-40]

Valcke S, Terray L, Piacentini A (2000) The OASIS Coupler User's Guide, Version 2.4. Technical Report TR/CGMC/00-10 CERFACS, p 85

Xu D, Malanotte-Rizzoli P (2013) Seasonal variation of the upper layer of the South China Sea and the Indonesian Seas: an Ocean Model Study. Dyn Atmos Oceans 63:103–130. doi:10.1016/j.dynatmoce.2013.05.002

Zeng X, Zhao M, Dickinson RE (1998) Intercomparison of bulk aerodynamic algorithms for the computation of sea surface fluxes using TOGA COARE and TAO data. J Climate 11:2628–2644

Zou L, Zhou T (2011) Sensitivity of a regional ocean-atmosphere coupled model to convection parameterization over western North Pacific. J Geophys Res 116:D18106. doi:10.1029/2011JD015844